Pathophysiology 26 (2019) 281–287

Contents lists available at ScienceDirect

Pathophysiology

journal homepage: www.elsevier.com/locate/pathophys

Effects of experimental intracerebral ventricular injection of amyloid beta peptide (1-42) aggregates on daily rhythms of Aβ-degrading enzymes in the hippocampus: Relevance to Alzheimer's disease pathophysiology

Andrea Castro, Cinthia Coria-Lucero, Ana Anzulovich*, Lorena Navigatore-Fonzo*

Laboratory of Chronobiology, Multidisciplinary Institute of Biological Research-San Luis (IMIBIO-SL), National Council of Science and Technology (CONICET), National University of San Luis (UNSL). Av Ejército de los Andes N°950, D5700HHW, San Luis, Argentina

ARTICLE INFO

Article history:
Received 17 January 2019
Received in revised form 24 June 2019
Accepted 27 July 2019

Keywords:
Neprilysin
Endothelin-converting enzyme
Insulin-degrading enzyme
Daily rhythm
Antioxidant enzymes
Alzheimer

ABSTRACT

One of the main pathological features in the Alzheimer disease (AD) is the presence of senile plaques, primarily composed of Aβ peptide aggregates, in cortex and hippocampus. AD late onset, which constitutes 90% of cases, could be mainly attributable to deficiencies in the clearance of the Aß peptide. Here we show that expression of Aβ-degrading enzymes varies on a daily basis in the hippocampus. Interestingly, an intracerebroventricular injection of Aβ aggregates modified temporal patterns of Aβ-degrading proteases, as well as clock proteins (BMAL1 and RORα) and antioxidant enzymes (CAT and GPx) daily rhythms. Our findings showed that the increase of Aβ leads to the alteration of the enzymes involved in the clearance, and, consequently, to an increase of oxidative stress and alteration of the cellular redox state, affecting the functioning of the endogenous clock and daily rhythms of BMAL1, RORα and their target genes, in this disease.

1. Introduction

Alzheimer's disease (AD), a progressive neurodegenerative disorder, is the most common form of irreversible dementia, among the elderly people. It is clinically characterized by progressive cognitive impairment, loss of memory and abnormal behavior [1,2].The main pathological features include the presence of neurofibrillary tangles (NFT) and senile plaques (SP), particularly, in cortex and hippocampus [3]. SPs are primarily composed of Aβ peptide aggregates. The Aβ peptide involved in the pathogenesis of the disease is produced by sequential cleavage of the amyloid precursor protein by β- and γ-secretases [4,5]. Late onset AD (LOAD) which constitutes 90% of cases could be mainly attributable to deficiencies in the clearance of the Aß peptide [4].

Enzymes with Aβ-degrading activity include members of the zinc metalloendopeptidase family. Among them, the ones with the most physiological relevance in the brain are neprilysin(NEP), endothelin-converting enzymes (ECE1 and ECE2) and insulin degrading enzyme (IDE) [6–9]. Research conducted by Eckman and collaborators [10,11] showed high levels of Aβ1-40 and 1-42 in the brain of ECE-2 knockout mice. In addition, a loss-of-function mutation of IDE causes cerebral accumulation of Aβ in rodents [12]. It has been also reported that NEP expression is reduced in the AD brain compared with age-matched control patients [13].

The oxidative stress also plays a central role in the development of AD [14,15]. Several evidences suggest that two key reactive oxygen species, hydrogen peroxide (H_2O_2) and the hydroxyl radical ($^{\bullet}OH$), are generated directly by Aβ (1–42) oligomers, and implicated in AD [16–18].Thus, postmortem studies in AD patients' brain have shown increased levels of proteins and lipids oxidation, and reduced activity of the antioxidant defense system [19,20]. Recently, we showed that an i.c.v. injection of Aβ aggregates modifies daily rhythms of lipoperoxidationan GSH levels in the rat hippocampus [21].In addition, multiple clinical studies have shown that disruption of sleep and circadian rhythms is one of the common and earliest signs of AD [22,23].

Abbreviations: AD, Alzheimer's disease; NFT, neurofibrillary tangles; SP, senile plaques; LOAD, Alzheimer's disease late onset; NEP, neprilysin; ECE, endothelin-converting enzymes; IDE, insulin degrading enzyme; SNC, suprachiasmatic nucleus; MDA, malondialdehyde; ZT, zeitgeber time; ANOVA, analysis of variance.

* Corresponding authors.
E-mail addresses: acanzu@unsl.edu.ar (A. Anzulovich), lnavigatore@unsl.edu.ar (L. Navigatore-Fonzo).

https://doi.org/10.1016/j.pathophys.2019.07.003
0928-4680/

Biological rhythms are generated by environmental time cue-entrained biological clocks. Environmental time cues are usually called '*zeitgebers*' (from German *zeit*: time and *geber*: giver, 'time giver'). Under natural conditions, the biological clock adjusts its period and phase to the predominant time cue or *zeitgeber*. Thus, the alternation between day and night is the strongest *zeitgeber* responsible for synchronizing the circadian timing system [24]. Chronobiologists name *zeitgeber* time (ZT) ZT0 when lights on in the animal facility and, from then, ZT1, ZT2, ZT3. . .ZT24to the following time points occurring afterwards. In mammals, the Circadian System generates circadian rhythms through a master clock in the suprachiasmatic nucleus (SCN), which receives the environmental signal through the retinohypothalamic tract and synchronizes rhythmic biological processes occurring in peripheral clocks located in most, if not all, organs and tissues. At the cellular level, circadian rhythms are generated by a complex interaction, and daily alternation, between clock transcription factors, such as BMAL1:CLOCK(activator) and PER:CRY (repressor) heterodimers, which constitute the molecular core clock machinery in most of the tissues. An accessory circuit made up of RORα and REVERB transcription factors, which, among others, regulates the oscillating expression of Bmal1, completes the cellular clock [25]. In our previous work, we also showed that an i.c.v. injection of Aβ aggregates phase shifts daily rhythms of putative cellular clock targets, such as Bdnf, Neurogranin and, the Aβ-clearance-related, ApoE, in the rat hippocampus [21].Considering above observations, in this work, we wonder, first, whether expression of Aβ-degrading proteases, NEP, ECE1 and IDE, oscillates rhythmically in the rat hippocampus, and second, which are the consequences of an i.c.v. injection of Aβ aggregates on daily patterns of cellular clock factors, Aβ-degrading enzymes, and antioxidant enzymes expression, in the rat hippocampus.

2. Materials and methods

2.1. Animal model

Three-month-old males Holtzman rats were used in this study. Groups were defined as: control (CO) and Aβ-injected (Aβ) (n = 12/group). Aβ (1-42) powder was dissolved in sterile saline solution (2 mg/mL) and incubated at 37 °C for 7 days to obtain the neurotoxic (aggregated) form [26].Animals were maintained under 12 h-light:12 h-dark lighting conditions and received water and food ad libitum. On the day of surgery, rats were anesthetized with ketamine hydrochloride (80 mg/kg) and xylazine (10 mg/kg) and placed in a stereotaxic apparatus. Under anesthetization, vehicle (saline solution) or Aβ aggregates (10 μg) were injected into the lateral ventricle (coordinates: AP:-1 mm, L:1.5 mm, and DV:-3.5 mm) of CO and Aβ rats, respectively (according to Zhang [27]. Seven days after surgery, three rats from each group were euthanized by decapitation every 6 h throughout a 24 -h period, at the *zeitgeber* time (ZT) points, namely, ZT2, ZT8, ZT14 and ZT20 (lights on at ZT0 and lights off at ZT12, in the animal facility).At ZT14 and ZT20 rats were euthanized under dim red light (0.1 lx) to avoid acute effects of light. All efforts were made to minimize animal suffering and to reduce the number of animals used.

2.2. Ethical approval

All experiments were carried out according to the National Institutes of Health Guide for the Care and Use of Laboratory Animals (NIH Publications No. 8023) and the National University of San Luis Committee' s Guidelines for the Care and Use of Experimental Animals (approved protocol Nº B-263/17).

2.3. Hippocampus dissection

Hippocampus samples were isolated every 6 h starting at ZT2 from CO and Aβ groups.

Hippocampi isolation was carried out as described in Babu [28]. Briefly, following animal decapitation, the head was obtained, and the skull was opened with sterile scissors. Brain was removed and cut along the longitudinal fissure to divide both hemispheres. The diencephalon was removed, and the hippocampus was resected from the neocortex and immediately placed in liquid nitrogen.

2.4. RNA isolation and Reverse Transcriptase (RT) reaction

Total RNA was extracted from hippocampus samples by using the Trizol reagent (Invitrogen Co) as directed by the manufacturers. The yield and purity of total RNA were determined spectrophotometrically at 260 and 280 nm. Gel electrophoresis and Gel-Red staining confirmed the integrity of the samples. Three micrograms of total RNA were reverse-transcribed with 200 units of MMLV Reverse Transcriptase (Promega Inc.) using random primer hexamers following the manufacturer's instructions [29].

2.5. PCR amplification

Fragments coding for 28S, NEP, IDE y ECE1 were amplified by PCR in 50 μl of reaction solution containing 0.2 mM dNTPs, 1.5 mM $MgCl_2$, 1.25U of Taq polymerase, and 50 pmol of each rat specific oligonucleotide primer and RT-generated cDNA (1/5 of RT reaction). The sequences of the specific primers used were: for NEP, forward (FW) primer 5′-AGCCGAAGAAGAAACAGCGA-3′ and reverse (RV) primer 5′-ACATTGCGTTTCAACCAGCC-3′ (fragment size 238 bp), for IDE, FW primer 5′- CAGCCATGAGTAAGCTGTGG-3′ and RV primer 5′-GGGTCCACATAAGCAAACGG -3′ (fragment size 100 bp), and for ECE1, FW primer 5′-CCCATGGTGAACGCCTACTA-3′ and RV primer 5′-GCCTTGATCGTCGAAAGCAT-3′ (fragment size 165 bp). In the case of NEP, samples were heated in a thermalcycler (My Cycler, BioRad, USA) to 94 °C for 2 min, followed by 30 cycles of (1) denaturation, 94 °C for 1 min; (2) annealing, 59 °C during 1 min; and (3) extension, 72 °C for 1 min. After 30 reaction cycles, the extension reaction was continued for 5 min. For IDE and ECE 1genes the thermalcycling conditions were similar but following 35 cycles of denaturation-annealing-extension. PCR products were then electrophoresed on 2% (w/v) agarose gel with 0.01% (w/v) GelRed™ (Biotium Inc., USA). The amplified fragments were visualized and photographed under ultraviolet transillumination. The mean of gray value for each band was measured using NIH ImageJ software (Image Processing and Analysis in Java from http://rsb.info.nih.gov/ij/) and the relative abundance of each band was normalized according to the housekeeping 28S gene, calculated as the ratio of the mean of gray value of each product to that of 28S [21].

2.6. Scanning of Aβ-degrading enzymes genes upstream regions for putative E-box and RORE sites

To identify putative clock-responsive (perfect E-box: CACGTG, or Ebox-like: CANNTG) and RORE, (A/G)GGTCA preceded by 6 pb A/T) DNA consensus regulatory sites, 2000 bp upstream of the translation start codon of NEP, IDE and ECE1 (NCBI GenBank Acc.#: NC_005101.4, NC_005100.4 and NC_005104.4,respectively) genes, were scanned for significant matches using the MatInspector® software from Genomatix (http://www.genomatix.de; Quandt et al. [30]).

2.7. Immunoblotting assays

Protein extracts were prepared from hippocampus samples obtained from each group of rats at the different ZTs during a 24-h period, in 120 mM KCl, 30 mM phosphate buffer, 1 μg/ml leupeptin and 1 μg/ml of pepstatin pH 7.2 at 4 °C. Aliquots containing 25 μg of total protein were subjected to electrophoresis in 12% polyacrylamide gels, and then transferred to Immobilon-PTM transfer membranes (Millipore, Bedford, MA). Briefly, membranes were blocked in Blotto (5% nonfat dry milk, 10 mM Tris-HCl, pH 8.0, and 150 mM NaCl) followed by 12 h overnight incubation at 10 °C with either goat anti-CAT, goat anti-GPx, or rabbit anti-BMAL, rabbit anti-RORα or anti-ACTIN antibodies (Abcam, USA), diluted 1:8000 in Blotto containing 0.05% thimerosal. After incubation with primary antibody, the membranes were washed in TBS (10 mM Tris-HCl, pH 8.0, and 150 mM NaCl) containing 0.05% Tween-20, before incubation with goat anti-rabbit IgG (Santa Cruz Biotechnology, Santa Cruz, CA) diluted 1:5000 in Blotto, for 2 h at room temperature. After washing, antibody/protein complexes were detected using a chemiluminescence method (Embiotec, Argentina) following the manufacturer's indications. The mean of intensity of each band was measured using the NIH ImageJ software (Image Processing and Analysis in Java from http://rsb.info.nih.gov/ij/). CAT, GPx, RORα and BMAL1 protein levels were normalized against ACTIN (endogenous control) [21].

2.8. Statistical analysis

Time point data were expressed as means ± standard errors of the mean (SE) and pertinent curves were drawn. Time series were computed by one-way ANOVA followed by Tukey's post-hoc test for specific comparisons. A $p < 0.05$ was considered to be significant. Daily rhythms were assessed by the Chronos-Fit software, using a combination of a partial Fourier analysis [31]. The percentage of rhythm (an index of the amount of variance accounted for) of the fitted curve, and the significance of rhythmicity, testing the null hypothesis of the amplitude being equal to zero, was performed using an F test (>3.5; $p < 0.05$). A cosine-fitted curve was generated with GraphPad Prism® 3.0 software (CA, USA). Student's *t*-test was used for comparison of mesor, amplitude or acrophase between CO and Aβ-injected groups, with $p < 0.05$ for significant differences.

3. Results

3.1. Daily profiles of Aβ clearance-related enzymes in the hippocampus. Effect of an i.c.v. injection of Aβ aggregates

First, we analyzed the daily expression of enzymes involved in the Aβ degradation, NEP, IDE and ECE1, in the rat hippocampus. All three enzymes' genes expression displays a daily and rhythmic pattern in that brain area (ANOVA $p < 0.0$ 1and Chronos-fit $p < 0.05$). The maximal level of NEP expression was observed at the beginning of the day (ZT 00:42 ± 00:08, $p < 0.01$) in the control group, while the highest levels of IDE and ECE1 transcripts occurred at the beginning of the night, ZT 14:40 ± 00:12 and ZT 15:17 ± 01:22, respectively ($p < 0.01$ in both cases). The i.c.v. injection of Aβ aggregates (1-42) had a differential effect on those daily patterns. On one hand, it phase shifted the NEP and IDE expression rhythms (from ZT 00:42 ± 00:08 to 17:36 ± 01:18, $p < 0.001$, for NEP, and from ZT 14:40 ± 00:12 to 10:55 ± 00:08, $p < 0.001$, for IDE). On the other hand, the i.c.v. injection of Aβ aggregates decreased the IDE expression rhythm's amplitude ($p < 0.05$) and increased the mesor of IDE and ECE1 mRNA levels oscillations ($p < 0.001$ and $p < 0.05$, respectively) in comparison to the CO group (Fig. 1, Table 1).

3.2. Putative E-box and RORE sites on NEP, IDE and ECE1 genes upstream region

Scanning of 2000 bp upstream of the translation start codon in the Genomatix database revealed one perfect E-box and six Ebox-like sites in the NEP gene upstream region, five E-box-like and two RORE elements in the IDE gene regulatory regions, and one perfect E-box, four E-box-like and three RORE sites in the ECE1 gene regulatory regions (Fig. 2).

3.3. Effect of an i.c.v. injection of Aβ aggregates on daily rhythms of clock proteins in the rat hippocampus

We observed BMAL1 and RORα levels vary significantly throughout a day, in the rat hippocampus (ANOVA, $p < 0.05$ and $p < 0.01$; Chronos-fit, $p < 0.05$ and $p < 0.05$, respectively) with maximal protein levels occurring at ZT 07:00 ± 00:24 and ZT 06:02 ± 00:17, respectively (Fig. 3, Table 2). The injection of Aβ aggregates exerted differential effects on the hippocampal clock

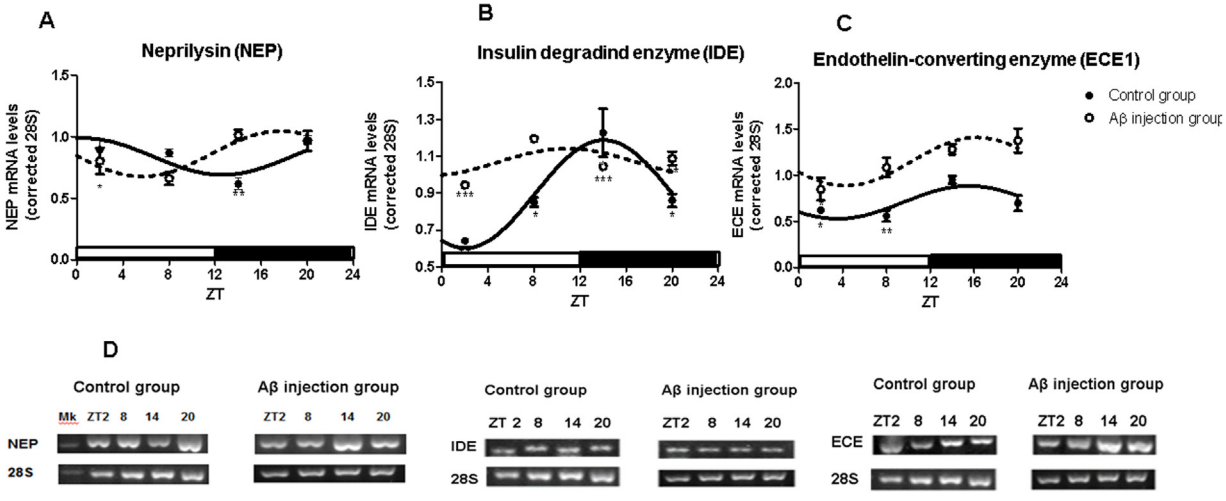

Fig. 1. Daily profiles of Aβ clearance-related enzymes in the hippocampus. Effect of an i.c.v. injection of Aβ aggregates. Each value on the curves represents the mean ± SEM of n = 3 hippocampus samples. Horizontal bars represent the distribution of light (open) and dark (closed) phases of the 24 h photoperiod. ZT is zeitgeber time, with ZT = 0 when light is on. Statistical analysis was performed using one-way ANOVA followed by Tukey test with *P < 0,05; **P < 0,01 and ***P < 0,001 when compared indicated means with the corresponding maximal value in each group. A cosine-fitted curve was generated with GraphPad Prism® 3.0 software (CA, USA). D) Representative patterns of PCR products at different ZTs throughout a daynight cycle (Mk: DNA Ladder).

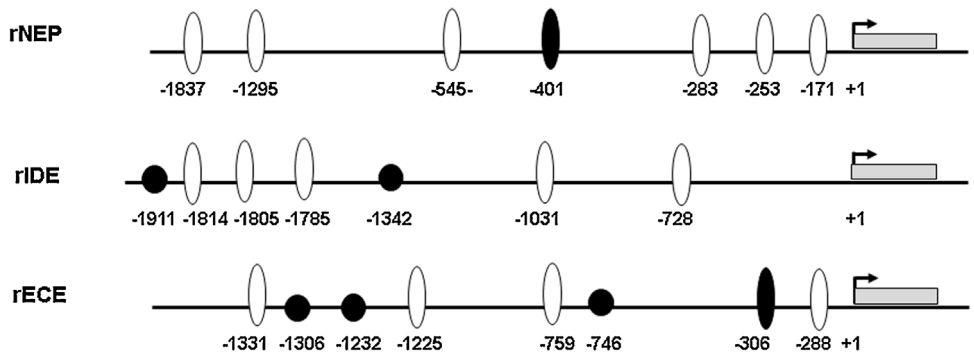

Fig. 2. Putative E-box and RORE sites on NEP, IDE and ECE1 genes upstream region. Arrows indicate the first translation codon, gray boxes represent exons, black circles are RORE sites, black ovals are perfect E-box, and white ovals are E-box-like sites. Negative (−) numbers indicate regulatory sites positions relative to the start of translation (+1).

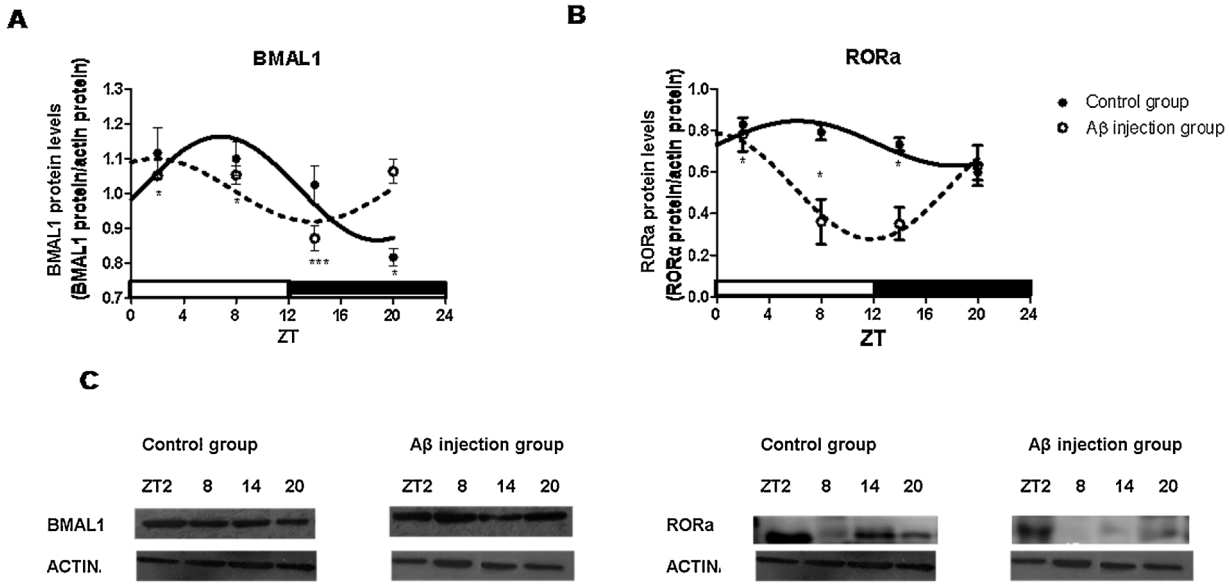

Fig. 3. Effect of Aβ aggregated on daily rhythms of clock proteins in the hippocampus rats Each point on the graphs represents the mean ± SEM of n = 3hippocampus samples. Horizontal bars represent the distribution of light (open) and dark (closed) phases of the 24 h photoperiod. ZT is zeitgeber time, with ZT = 0 when light is on. Statistical analysis was performed using one-way ANOVA followed by Tukey test with *P < 0,05; and ***P < 0,001 when compared indicated means with the corresponding maximal value in each group. A cosine-fitted curve was generated with GraphPad Prism® 3.0 software (CA, USA). C) Representative immunoblots of daily BMAL1 and RORα protein levels.

Table 1
Rhythms' parameters of NEP, IDE and ECE1 oscillating mRNA levels in the hippocampus of control and Aβ-injected groups.

Rhythm Parameters	Control group (mean ± SEM)	Aβ-injected group (mean ± SEM)	p
NEP mRNA levels			
MESOR	0.84 ± 0.02	0.86 ± 0.04	N/S
AMPLITUDE	0.15 ± 0.03	0.20 ± 0.01	N/S
ACROPHASE	00:42 ± 00:08	17:36 ± 01:18	<0.001
IDE mRNA levels			
MESOR	0.89 ± 0.02	1.07 ± 0.03	<0.001
AMPLITUDE	0.29 ± 0.06	0.09 ± 0.01	<0.05
ACROPHASE	14:40 ± 00:12	10:55 ± 00:08	<0.001
ECE1 mRNA levels			
MESOR	0.70 ± 0.01	1.15 ± 0.10	<0.05
AMPLITUDE	0.20 ± 0.04	0.26 ± 0.02	N/S
ACROPHASE	15:17 ± 01:22	16:19 ± 00:27	N/S

Note: Data are presented as mean ± SEM (n = 3 per group). p-levels were obtained for the corresponding control vs. Aβ-injected groups comparisons using Student's *t*-test.
N/S = not significant.
NEP levels (% rhythm Control group: 48.96Aβ injected group: 68.37).
IDE levels(% rhythm Control group: 51.41 Aβ injected group: 78.32).
ECE1 levels (%rhythm Control group: 54.71 Aβ injected group: 53.09).

proteins rhythms. Thus, Aβ injection phase advanced BMAL1 oscillating expression (from ZT 07:00 ± 00:24 to ZT 01:24 ± 01:00, p < 0,05) without affecting the rhythm's amplitude or mesor, on one hand,and it phase delayed RORα protein rhythmicity (from ZT 06:02 ± 00:17 to ZT 00:05 ± 00:29, p < 0.01), reduced the mesor and increased the rhythm's amplitude, on the other (p < 0.01 and p < 0.05, respectively; Fig. 3 and Table 2).

3.4. Daily profiles of CAT and GPx protein levels in the hippocampus of Aβ-injected rats

The results revealed that CAT levels follow a robust diurnal rhythm in the hippocampus of control rats (ANOVA p < 0.05 and Chronos-fit p < 0.05), with the highest level occurring at ZT 01:58 ± 00:11. The i.c.v. injection of Aβ aggregates phase-shifted daily rhythm of CAT (ZT 01:58 ± 00:11 to ZT 20:51 ZT ± 00:35 (p < 0.05) and decreased the rhythm's mesor (0.79 ± 0.04 vs 0.65 ± 0.01, p < 0.05) in the rat hippocampus (Fig. 4 and Table 3). On the other hand, we observed also GPx protein levels displays a 24-h rhythm in the rat hippocampus (ANOVA p < 0.05 and Chronos-fit p < 0.05) peaking towards the middle of the day (ZT 12:30 ± 01:28) in the control. The Aβ-injected group showed a phase delay in GPx rhythm's, from ZT 12:30 ± 01:28 to ZT 21:23 ± 00:43 (p < 0.01)

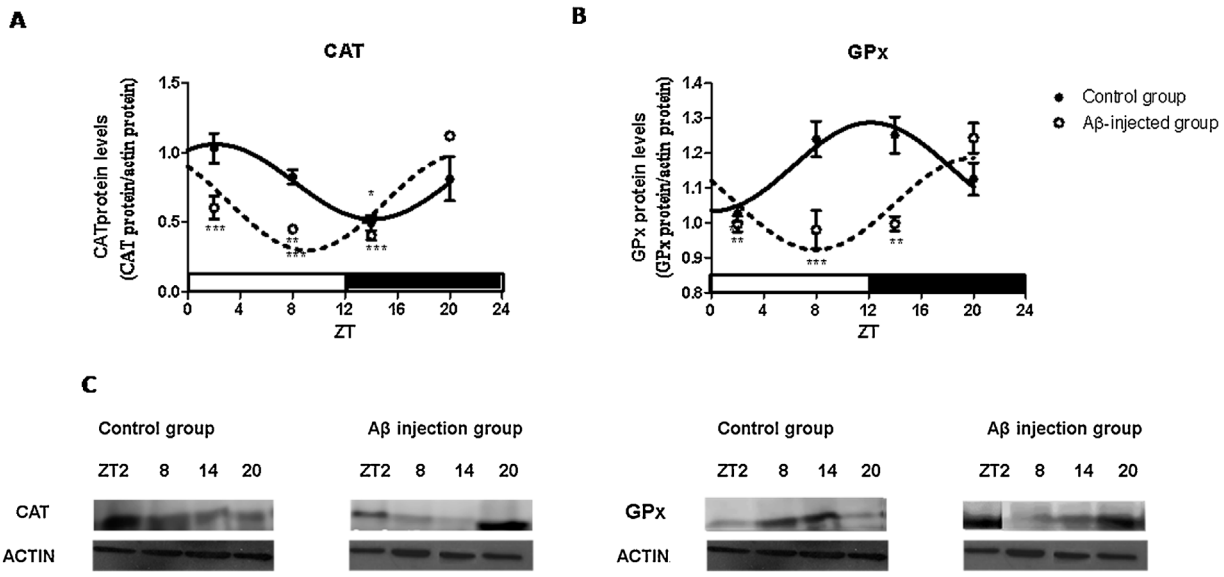

Fig. 4. Daily profiles of CAT and GPx protein levels in the hippocampus of Aβ-injected rats Each point on the graphs represents the mean ± SEM of n = 3 hippocampus samples. Horizontal bars represent the distribution of light (open) and dark (closed) phases of the 24 h photoperiod. ZT is zeitgeber time, with ZT = 0 when light is on. Statistical analysis was performed using one-way ANOVA followed by Tukey test with *P < 0,05; **P < 0,01 and ***P < 0,001 when compared indicated means with the corresponding maximal value in each group. A cosine-fitted curve was generated with GraphPad Prism® 3.0 software (CA, USA). C) Representative immunoblots of daily CAT and GPx protein levels.

Table 2
Rhythms' parameters of BMAL1 and RORα oscillating protein levels in the hippocampus of control and Aβ-injected groups.

Rhythm Parameters	Control group (mean ± SEM)	Aβ-injected group (mean ± SEM)	p
BMAL1 protein levels			
MESOR	1.02 ± 0.04	1.02 ± 0.00	N/S
AMPLITUDE	0.15 ± 0.04	0.11 ± 0.02	N/S
ACROPHASE	07:00 ± 00:24	01:24 ± 01:00	<0.05
RORα protein levels			
MESOR	0.74 ± 0.01	0.53 ± 0.04	<0.01
AMPLITUDE	0.11 ± 0.04	0.30 ± 0.04	<0.05
ACROPHASE	06:02 ± 00:17	00:05 ± 00:29	<0.01

Note: Data are presented as mean ± SEM (n = 3 per group). p-levels were obtained for the corresponding control vs. Aβ-injected groups comparisons using Student's *t*-test.
N/S = not significant.
BMAL1 levels (% rhythm Control group: 55.56Aβ injected group: 49.88).
RORα levels (% rhythm Control group: 60.56 Aβ injected group: 67.28).

Table 3
Rhythms' parameters of CAT and GPx oscillating protein levels in the hippocampus of control and Aβ-injected groups.

Rhythm Parameters	Control group (mean ± SEM)	Aβ-injected group (mean ± SEM)	p
CAT protein levels			
MESOR	0.79 ± 0.04	0.65 ± 0.01	<0.05
AMPLITUDE	0.30 ± 0.04	0.35 ± 0.02	N/S
ACROPHASE	01:58 ± 00:11	20:51 ± 00:35	<0.05
GPx protein levels			
MESOR	1.17 ± 0.01	1.06 ± 0.01	<0.01
AMPLITUDE	0.11 ± 0.05	0.13 ± 0.06	N/S
ACROPHASE	12:30 ± 01:28	21:23 ± 00:43	<0.01

Note: Data are presented as mean ± SEM (n = 3 per group). p-levels were obtained for the corresponding control vs. Aβ-injected groups comparisons using Student's *t*-test.
N/S = not significant.
CAT levels (% rhythm Control group: 63.57Aβ injected group: 71.07).
GPx levels (% rhythm Control group: 61.80 Aβ injected group: 58.81).

and a decrease in the mesor of rhythms (1.17 ± 0.01 vs 1.06 ± 0.01, p < 0.01) compared with controls.

4. Discussion

Recent results from our group revealed that Aβ levels vary on a daily basis in the rat hippocampus, with the maximum level of Aβ occurring around the middle of the light period [21]. These observations led us to question whether the enzymes involved in the clearance of Aβ move in time with the cellular clock in the rat hippocampus and, secondly, which could be the effects of an i.c.v. injection of Aβ aggregates on the temporal organization of the Aβ hippocampal clearance. Thus, herein, and for the first time in our knowledge, we show that NEP, IDE and ECE1 expression displays daily rhythms in the rat hippocampus. Interestingly, an i.c.v. injection of Aβ aggregates modified temporal patterns of Aβ-degrading proteases.

Neprilysin, IDE and ECE1 expression was analyzed throughout the day in the hippocampus of rats maintained under light:dark (LD) conditions. In fact, we observed that transcript levels of enzymes involved in Aβ clearance exhibit a daily rhythmicity in rat hippocampus, with the NEP expression peaking at the beginning of the day and the highest levels of IDE and ECE1 transcripts occurring at the beginning of the night (Fig. 1 and Table 1). To date, we have not found any other study on daily rhythms of those proteases in the hippocampus, nor in other brain tissues; however, some studies show an association between IDE or NEP and the circadian clock, in different animal models and tissues [32,33]. Thus, Zhao and collaborators [32] show a day-night variation of IDE expression in the liver of mouse, which is lost in mice lacking the clock's Per2 factor. On the other hand, Isaac and collaborators [33] propose a role for NEP as a regulator of the circadian signal in Drosophila, since this endopeptidase was able to hydrolyze and inactivate the pigment dispersing factor, a key neurotransmitter in the regulation of the circadian rhythm of locomotor activity of this species.

Daily rhythms of NEP, IDE and ECE1 expression suggest a temporally well-orchestrated Aβ-clearance in the hippocampus. The NEP expression peak occurring at the beginning of the day precedes, probably in a context of predictive homeostasis, the Aβ rhythm's acrophase (at ZT08:24 ± 00:39), observed previously by us [21], in the rat hippocampus. On the other hand, maximal expression of IDE and ECE precedes Aβ rhythm's nadir during the night period. Such organization might ensure that the maximal levels of Aβ occur

at the second half of the day. Noteworthy, a number of memory and learning tasks related to synaptic plasticity, involving working memory or LTP in the hippocampus, occur mainly during the diurnal phase [34] and accumulating evidence suggests Aβ has important physiological functions such as modulation of synaptic plasticity and neuroprotection [35].

Daily rhythms of NEP, IDE and ECE1 expression suggested us that genes encoding those enzymes could be under the control of the endogenous clock. Our bioinformatic analysis revealed the presence of clock-responsive E-box sites in regulatory regions of NEP, IDE and ECE1 genes as well as ROR/REVERB-responsive, RORE, sites in the regulatory regions of IDE and ECE1 genes (Fig. 2). Such findings led us to investigate the temporal variation of clock factors, BMAL1 and RORα, protein levels, in the rat hippocampus.

In this study, we observed BMAL1 protein levels vary throughout a 24 -h cycle, with their maximum occurring at the middle of the day, preceding IDE and ECE1 expression peaks, in the hippocampus of control rats. As expected, we also observed RORα protein rhythm's acrophase precedes BMAL1 protein peak, as well as IDE and ECE1 maximal expression. A relationship between the cellular clock and IDE expression levels has been reported by Zhao et al. [32] who showed that hepatic IDE displays a day and night rhythm, which is impaired in mPer2-deficient mice. Ours and their observations led us to propose that exist a daily organization in the IDE- and ECE1-mediated Aβ clearance, probably orchestrated by the endogenous local clock in the hippocampus. On the contrary, we couldn't establish a temporal relationship between the NEP expression and the rhythmicity of clock activators, BMAL1 and RORα. Such discrepancy could be explained, at least in part, for the absence of RORE sites in the NEP regulatory region. In addition, considering that Nakahata et al [36] reported that Ebox-like sites should be in tandem to be functional and regulate the circadian oscillation, other reason might be the fact that E-box-like sites in the NEP regulatory region are spaced by several nucleotides. Moreover, it has been shown, Ebox sites could be targets for other transcription factors such as, for example, SREBP. Knowing NEP participates also in the SREBP proteolysis, it wouldn't be odd the transcription factor regulates NEP expression, in a feedback way [37]. In this case, SREBP would compete with BMAL1:CLOCK for the binding to the Ebox sites. On the other hand, on the contrary to IDE and ECE, NEP gene transcription is also epigenetically regulated by HDAT1.

Although other researchers have shown an effect of bilateral injection in the hippocampus of soluble beta-amyloid peptide 1–42 (Ab1–42), on the NEP and IDE protein levels [38,39], this would be, at least to our knowledge, the first work that investigates the consequences of an i.c.v. injection of Aβ aggregates on the daily rhythmicity of enzymes involved in the clearance of amyloid deposits, in the hippocampus. Interestingly, we observed that Aβ aggregates exerted differential effects on the NEP, IDE and ECE1 daily rhythms, modifying either their phase, mesor or amplitude. Particularly, Aβ aggregates delayed the NEP rhythm's acrophase, advanced the IDE rhythm's acrophase, reduced its amplitude and increases IDE and ECE rhythm's mesor. Interestingly, we also observed that the i.c.v. injection of Aβ aggregates modifies BMAL1 and RORα protein rhythms in the rat hippocampus, causing a 6h-advance of BMAL1 as well as RORα daily peaks. To date, we did not find studies on the consequences of an i.c.v injection of aggregated Aβ (1-42) on daily rhythms of clock proteins. However, studies carried out by Wilkaniec et al. [40] showed that circadian rhythms of clock genes expression were abolished by Aβ peptides in human primary skin fibroblasts. This would be, somehow, in line with the reduced RORα rhythm's mesor observed in the hippocampus of our experimental animals. In addition, Wang et al. [41], showed that Aβ 31-35 administered into the hippocampus, altered the expression of the Per1 and Per2 in the SCN, hippocampus and heart.

Noteworthy, in this study, IDE rhythm's acrophase was advanced in the same way than BMAL1 and RORa rhythms' acrophases following the i.c.v. injection of the Aβ aggregates. On the other hand, the increase of IDE and ECE rhythm's mesor observed here, in the hippocampus of Aβ-injected rats, would be consistent with Chang and collaborators [42] who demonstrated that Aβ 1-42 injection significantly increases IDE and NEP levels in the mouse hippocampus and cortex. Higher IDE and ECE rhythms' mesor might be an adaptative response to the increased hippocampal Aβ content showed by us in Navigatore-Fonzo et al. [21].

Numerous studies have shown that increased oxidative stress plays an important role in the etiology and progression of AD. Additionally, it has been shown that injection of Aβ induce oxidative stress, cognitive dysfunction and impairing memory in rat [43–45].Our investigations have shown that an i.c.v injection of aggregated Aβ (1-42) induces oxidative damage. Particularly, we found that an injection of Aβ aggregates caused a phase shift, and increase the rhythm's mesor of lipoperoxidation levels in the rat hippocampus [21].

It is well known that CAT eliminates H_2O_2, by reducing it to water and oxygen, and that GPx helps to prevent the formation of hydrogen and organic hydroperoxides, thus protecting the cell from damaging effects of free radicals. Interestingly, we observed CAT and GPx protein levels vary throughout a 24 h period, peaking at the beginning of the day and the night, respectively, in the rat hippocampus (Fig. 4 and Table 3). Rhythms of CAT and GPx have also been observed by us and others in the rat brain [29,46,47]. As expected, temporal patterns observed in the rat hippocampus were consistent with the rhythm of lipoperoxidation observed previously [21]. Thus, the highest level of CAT and GPx precedes the nocturnal peak of malondialdehyde (MDA, ZT 19:48 ± 00:54) in the context of predictive homeostasis.

Interestingly, in the present study, we found, for the first time in our knowledge, that an i.c.v injection of Aβ aggregates caused a phase shift and decreased the rhythm's mesor of CAT and GPx levels in the rat hippocampus (Fig. 4 and Table 3). Even though, to date, we did not find studies on the consequences of an i.c.v injection of aggregated Aβ (1-42) on daily rhythms of antioxidant enzymes, some studies carried out by Pan et al. [48] have shown that an injection of Aβ(1–42) decreased the levels of CAT and GPx in the rat brain.

In conclusion, here we describe the temporal organization of hippocampal Aβ clearance-related events with the clock RORα and BMAL1 protein rhythms' acrophases preceding nocturnal peaks of IDE and ECE1 expression. In addition, maximal NEP expression precede Aβ protein peak occurring on the second half of the day, as showed in Navigatore Fonzo et al. [21], probably, in the context of predictive homeostasis. However, the maximal levels of IDE and ECE1 expression occurring after the Aβ protein peak, could be explain in terms of reactive response. Maximal levels of TBARS (shown in our previous work) follow the peak of Aβ, coinciding with the lowest level of CAT and GPx, which confirms the role of amyloid peptide as a trigger for oxidative stress.

Our findings showed that the increase of Aβ leads to the alteration of the enzymes involved in the clearance, and, consequently, to an increase of oxidative stress and alteration of the cellular redox state, affecting the functioning of the endogenous clock and daily rhythms of BMAL1, RORα and their target genes, in this disease.

Funding

This work was supported by the Florencio Fiorini Foundation (Buenos Aires, Argentina) for 2013–2014 years and by the National University of San Luis (UNSL, Argentina) through the PROICO 2-0518 grant.

Declaration of Competing Interest

The authors have no conflicts of interest. The authors are solely responsible for the contents and writing of the paper.

Acknowledgments

We thank to Mr Gerardo Randazzo from the Department of Biological Chemistry for his assistance throughout the period of this research work.

References

[1] S. Mehan, R. Arora, V. Sehgal, Inflammatory diseases –immunopathology, clinical and pharmacological bases, in: M. Khatami (Ed.), Dementia: A Complete Literature Review on Various Mechanisms Involved in Pathogenesis and an Intracerebroventricular Streptozotocin-Induced Alzheimer's Disease, vol. 2, InTech, Rijeka, 2012, pp. 3–19.
[2] A. Khorrami, S. Ghanbarzadeh, J. Mahmoudi, A. Nayebi, N. Maleki-Dizaji, A. Garjani, Investigation of the memory impairment in rats fed with oxidized-cholesterol-rich diet employing passive avoidance test, Drug Res. (Stuttg.) 65 (2014) 231–237.
[3] H. Querfurth, F. LaFerla, Alzheimer's disease, N. Engl. J. Med. 362 (2010) 329–344.
[4] D. Selkoe, Alzheimer's disease: genes, proteins, and therapy, Physiol. Rev. 81 (2001) 741–766.
[5] M. Mattson, Pathways towards and away from Alzheimer's disease, Nature 430 (2004) 631–639.
[6] S. El-Amouri, H. Zhu, J. Yu, R. Marr, I. Verma, M. Kindy, Neprilysin: an enzyme candidate to slow the progression of Alzheimer's disease, Am. J. Pathol. 172 (2008) 342–354.
[7] E. Eckman, C. Eckman, Aβ-degrading enzymes: modulators of Alzheimer's disease pathogenesis and targets for therapeutic intervention, Biochem. Soc. Trans. 33 (2005) 101–105.
[8] R. Isaac, E. Johnson, N. Audsley, A. Shirras, Metabolic inactivation of the circadian transmitter, pigment dispersing factor (PDF), by neprilysin-like peptidases in Drosophila, J. Exp. Biol. 210 (2001) 465–470.
[9] M. Leissring, W. Farris, A. Chang, D. Walsh, X. Wu, X. Sun, M. Frosch, D. Selkoe, Enhanced proteolysis of β-amyloid in APP transgenic mice prevents plaque formation, secondary pathology and premature death, Neuron 40 (2003) 87–93.
[10] E. Eckman, M. Watson, L. Marlow, K. Sambamurti, C. Eckman, Alzheimer's disease β-amyloid peptide is increased in mice deficient in endothelin-converting enzyme, J. Biol. Chem. 278 (2003) 081–084.
[11] E. Eckman, S. Adams, F. Troendle, B. Stodola, M. Kahn, A. Fauq, H. Xiao, K. Bernstein, C. Eckman, Regulation of steady-state b-amyloid levels in the brain by neprilysin and endothelin-converting enzyme but not angiotensin-converting enzyme, J. Biol. Chem. 281 (2006) 471–478.
[12] Y. Shen, A. Joachimiak, M. Rosner, W. Tang, Structures of human insulin-degrading enzyme reveal a new substrate recognition mechanism, Nature 443 (2006) 870–874.
[13] N. Nalivaeva, L. Fisk, E. Kochkina, S. Plesneva, I. Zhuravin, E. Babusikova, D. Dobrota, A. Turner, Effect of hypoxia/ischemia and hypoxic preconditioning/reperfusion on expression of some amyloid-degrading enzymes, Ann. N.-Y. Acad. Sci. 1035 (2004) 21–33.
[14] F. Copped, L. Migliore, DNA damage and repair in Alzheimer's disease, Curr. Alzheimer Res. 6 (2009) 36–47.
[15] B. Uttara, A. Singh, P. Zamboni, R. Mahajan, Oxidative Stress and Neurodegenerative diseases: a review of upstream and downstream antioxidant therapeutic options, Curr. Neuropharmacol. 7 (2009) 65–74.
[16] X. Huang, M. Cuajungco, C. Atwood, M. Hartshorn, J. Tyndall, G. Hanson, K. Stokes, M. Leopold, G. Multhaup, L. Goldstein, R. Scarpa, Cu(II) potentiation of Alzheimer abeta neurotoxicity. Correlation with cell-free hydrogen peroxide production and metal reduction, J. Biol. Chem. 274 (1999) 11–16.
[17] G. Perry, A. Cash, M. Smith, Alzheimer disease and oxidative stress, J. Biomed. Biotechnol. 2 (2002) 120–123.
[18] B. Tabner, J. Mayes, D. Allsop, Hypothesis: soluble Aβ oligomers in association with redox-active metal ions are the optimal generators of reactive oxygen species in Alzheimer's disease, Int. J. Alzheimers Dis. (2011) 1–6.
[19] P. Mao, P. Reddy, Aging and amyloid beta-induced oxidative DNA damage and mitochondrial dysfunction in Alzheimer's disease: implications for early intervention and therapeutics, Biochim. Biophys. Acta: Mol. Basis Dis. 1812 (2011) 59–70.
[20] E. Mutisya, A. Bowling, M. Beal, Cortical cytochrome oxidase activity is reduced in Alzheimer's disease, J. Neurochem. 63 (1994) 79–84.
[21] L. Navigatore-Fonzo, A. Castro, V. Pignataro, M. Casais, M. Garraza, A. Anzulovich, Daily rhythms of cognition-related factors are modified in an experimental model of Alzheimer disease, Brain Res. 1660 (2017) 27–35.
[22] Y. Ju, B. Lucey, D. Holtzman, Sleep and Alzheimer disease pathology–a bidirectional relationship, Nat. Rev. Neurol. 10 (2014) 115–119.
[23] K. Wulff, S. Gatti, J. Wettstein, R. Foster, Sleep and circadian rhythm disruption in psychiatric and neurodegenerative disease, Nat. Rev. Neurosci. 11 (2010) 589–599.
[24] D. Golombek, R. Rosenstein, Physiology of circadian entrainment, Physiol. Rev. 90 (2010) 063–102.
[25] J. Mohawk, C. Green, J. Takahashi, Central and peripheral circadian clocks in mammals, Annu. Rev. Neurosci. 35 (2012) 445–462.
[26] W. Wang, W. Wang, G. Yao, Q. Ren, D. Wang, Z. Wang, P. Liu, P. Gao, Y. Zhang, S. Wang, S. Song, Novel sarsasapogenin-triazolyl hybrids as potential anti-Alzheimer's agents: design, synthesis and biological evaluation, Eur. J. Med. Chem. 151 (May (10)) (2018) 351–362.
[27] Y. Zhang, Y. Fan, M. Wang, D. Wang, X. Li, Atorvastatin attenuates the production of IL-1β, IL-6, and TNF-α in the hippocampus of an amyloid β1-42-induced rat model of Alzheimer's disease, Clin. Interv. Aging 8 (2013) 103–110.
[28] H. Babu, J. Claasen, S. Kannan, A. Rünker, T. Palmer, G. Kempermann, A protocol for isolation and enriched monolayer cultivation of neural precursor cells from mouse dentate gyrus, Front. Neurosci. 5 (2011) 89.
[29] L.S. Fonzo, R. Golini, S.M. Delgado, M.R. Bonomi, I.G. Rezza, M.S. Gimenez, A.C. Anzulovich, Temporal patterns of lipoperoxidation and antioxidant enzymes are modified in the hippocampus of vitamin A-deficient rats, Hippocampus (2009) 869–880.
[30] K. Quandt, K. Frech, H. Karas, E. Wingender, T. Werner, MatInd and MatInspector: new fast and versatile tools for detection of consensus matches in nucleotide sequence data, Nucleic Acids Res. 23 (1995) 878–884.
[31] P. Zuther, K. Witte, B. Lemmer, ABPM-FIT and CV-SORT: an easy-to-use software package for detailed analysis of data from ambulatory blood pressure monitoring, Blood Press. Monit. 1 (1996) 347–354.
[32] Y. Zhao, Y. Zhang, M. Zhou, S. Wang, Z. Hua, J. Zhang, Loss of mPer2 increases plasma insulin levels by enhanced glucose-stimulated insulin secretion and impaired insulin clearance in mice, FEBS Lett. 7 (2012) 06–11.
[33] R. Isaac, E. Johnson, N. Audsley, A. Shirras, Metabolic inactivation of the circadian transmitter, pigment dispersing factor (PDF), by neprilysin-like peptidases in Drosophila, J. Exp. Biol. 210 (2007) 465–470.
[34] O. Rawashdeh O, R. Parsons, E. Maronde, Clocking in time to gate memory processes: the circadian clock is part of the ins and outs of memory, Neural Plast (2018) 1–11.
[35] H. Pearson, C. Peers, Physiological roles for amyloid beta peptides, J. Physiol. (2006) 5–10.
[36] Y. Nakahata, M. Yoshida, A. Takano, H. Soma, T. Yamamoto, A. Yasuda, T. Nakatsu, T. Takumi, A direct repeat of E-box-like elements is required for cell-autonomous circadian rhythm of clock genes, BMC Mol. Biol. (2008) 8–12.
[37] M. Yamaguchi, H. Shirai, R. Sato, Y. Kawabe, R. Fukuda, T. Kodama, T. Hamakubo, Characterization of cleavage enzymes for sterol regulatory element binding protein in hamster liver microsomes, Biochem. Biophys. Res. Commun. (1999) 542–547.
[38] Q. Quan, J. Wang, X. Li, W. Wang, Ginsenoside Rg1 decreases Ab1–42 level by upregulating PPARc and IDE expression in the Hippocampus of a rat model of Alzheimer's disease, PLoS One 8 (2013), e59155, http://dx.doi.org/10.1371/journal.pone.0059155.
[39] H. Yuan, X. Li, Q. Quan, N. Wang, Y. Li, M. Li, Effects of Naoerkang on expressions of beta-amyloid peptide 1-42 and neprilysin in hippocampus in a rat model of Alzheimer's disease, Zhong Xi Yi Jie He Xue Bao 8 (2010) 152–157.
[40] A. Wilkaniec, K. Schmitt, A. Grimm, J. Strosznajder, A. Eckert, Alzheimer's amyloid-β peptide disturbs P2X7 receptor-mediated circadian oscillations of intracellular calcium, Folia Neuropathol. 54 (2016) 360–368.
[41] X. Wang, L. Wang, Q. Yu, L. Zhang, X. Zhao, X. Cao, Y. Li, Y. Li, Alterations in the expression of Per1 and Per2induced by Aβ 31-35 in the suprachiasmatic nucleus, hippocampus, and heart of C57BL7/6mouse, Brain Res. 1 (2016) 42–51.
[42] K. Chang, H. Zong, K. Ma, W. Zhai, W. Yang, X. Hu, J. Xu, X. Chen, S. Ji, Y. Qian, Activation of α7 nicotinic acetylcholine receptor alleviates Aβ1-42-induced neurotoxicity via downregulation of p38 and JNK MAPK signaling pathways, Neurochem. Int. 120 (2018) 238–250.
[43] H. Cai, C. Hölscher, X. Yue, S. Zhang, X. Wang, F. Qiao, W. Yang, J. Qi, Lixisenatide rescues spatial memory and synaptic plasticity from amyloid β protein-induced impairments in rats, Neuroscience 26 (2014) 6–13.
[44] W. Klein, W. Stine, D. Teplow, Small assemblies of unmodified amyloid beta-protein are the proximate neurotoxin in Alzheimer's disease, Neurobiol. Aging 25 (2004) 569–580.
[45] J. Wang, L. Ho, W. Zhao, K. Ono, C. Rosensweig, L. Chen, N. Humala, D. Teplow, G. Pasinetti, Grape-derived polyphenolics prevent Abeta oligomerization and attenuate cognitive deterioration in a mouse model of Alzheimer's disease, J. Neurosci. 18 (2008) 388–392.
[46] B. Escribano, A. Díaz-Moreno, I. Tasset, I. Túnez, Impact of light/dark cycle patterns on oxidative stress in an adriamycin-induced nephropathy model in rats, PLoS One 9 (5) (2014), e97713, http://dx.doi.org/10.1371/journal.pone.0097713, 22.
[47] V. Jiménez-Ortega, D. Cardinali, M. Fernández-Mateos, M. Ríos-Lugo, P. Scacchi, A. Esquifino, Effect of cadmium on 24-hour pattern in expression of redox enzyme and clock genes in rat medial basal hypothalamus, Biometals 23 (2010) 327–337.
[48] Y. Pan, X. Jia, E. Song, X. Peng, AstragalosideIV protects against Aβ1-42-induced oxidative stress, neuroinflammation and cognitive impairment in rats, Chin. Med. Sci. J. 30 (2018) 29–37.